Exp. Anim. 67(3), 373–382, 2018

—Original—

STF-083010, an inhibitor of XBP1 splicing, attenuates acute renal failure in rats by suppressing endoplasmic reticulum stress-induced apoptosis and inflammation

Lei LIU[1,2)]*, Lu XU[3)]*, Shaoqing ZHANG[2)], Dong WANG[4)], Guoxia DONG[2)], Hanwen CHEN[2)], Xinjian LI[4)], Chi SHU[5)], and Rong WANG[1)]

[1)]*Department of Nephrology, Shandong Provincial Hospital Affiliated to Shandong University, 324 Jingwuweiqi Road, Jinan, Shandong 250021, P.R. China*
[2)]*Department of General Practice, The Affiliated Hospital of Jining Medical University, 89 Guhuai Road, Jining, Shandong 272000, P.R. China*
[3)]*Department of Blood Purification, The Affiliated Hospital of Jining Medical University, 89 Guhuai Road, Jining, Shandong 272000, P.R. China*
[4)]*Department of Nephrology, The Affiliated Hospital of Jining Medical University, 89 Guhuai Road, Jining, Shandong 272000, P.R. China*
[5)]*High-tech Zone Laboratory of Public Test and Analysis Service, 18-32 Puhe Road, Shenyang 110179, P.R. China*

Abstract: Endoplasmic reticulum (ER) stress is one of the driving forces of ischemia/reperfusion (IR)-induced acute renal failure (ARF). STF-083010, an inhibitor of the endonuclease activity of inositol-requiring enzyme-1 (IRE1), has the potential to block the initiation of a prolonged unfolded protein response (UPR) that is stimulated by ER stress and alleviates the impairments due to ER stress. In the current study, it was hypothesized that STF-083010 was capable of ameliorating ER stress-related damages in IR-induced ARF. Rats were administrated with STF-083010 and were subjected to induction of ARF using a ligation method. Then the effect of STF-083010 administration on the renal structure and function, oxidative stress, and inflammation in model rats was assessed. Furthermore, the levels of expression of UPR members and downstream effectors regulating apoptosis were detected as well. The results showed that establishment of the ARF model induced ER stress and impaired the renal structure and function. Administration of STF-083010 ameliorated impairments in the structure and function of the kidneys and the effect was associated with the suppressed oxidative stress and inflammation. At the molecular level, STF-083010 inhibited the prolonged UPR by downregulating the expressions of GRP78, p-IRE1, XBP1s, CHOP, and caspase 3, partially explaining the decreased apoptotic rate. The current study evaluated the potential of STF-083010 in treating ER stress-induced symptoms in ARF for the first time, and the findings demonstrated that STF-083010 resulted in effective treatment outcomes of ARF.

Key words: acute renal failure, endoplasmic reticulum stress, inositol-requiring enzyme-1, STF-083010, unfolded protein response

(Received 18 October 2017 / Accepted 26 March 2018 / Published online in J-STAGE 25 April 2018)

Addresses corresponding: R. Wang, Department of Nephrology, Shandong Provincial Hospital Affiliated to Shandong University, 324 Jingwuweiqi Road, Jinan, Shandong 250021, P.R. China

**Lei Liu and Lu Xu contributed equally to this study.*

Supplementary Figure and Table: refer to J-STAGE: https://www.jstage.jst.go.jp/browse/expanim

Introduction

Acute renal failure (ARF) is characterized by the rapid decline of renal function [29] and commonly occurs in hospitalized patients, particularly in those with multi-organ failures. Worse still, the occurrence of ARF *per se* will increase the death risk of patients by 10- to 15-fold [5]. Therefore, poor situations associated with ARF make it imperative to explore novel treatment modalities for the disorder.

Ischemia-reperfusion (IR) injury is a major causal factor of ARF [20] and induces functional and structural deteriorations in endothelium and proximal tubule cells in the kidneys [3, 15, 18], leading to loss of cell to cell attachments, generation of reactive oxygen species (ROS), cell apoptosis and necrosis, and inflammatory responses [3, 15, 18]. Among the above events, apoptosis and inflammation have been conceived to play important roles in the pathophysiology of ARF [20]. Growing evidence shows that pro-inflammatory cytokine release, inflammatory cell recruitment, and mitochondrial dysfunction-induced apoptosis are implicated in the progression of kidney disorders [8, 9, 19]. Several mechanisms have been proposed to underlie the apoptosis and inflammation associated with ARF. Endoplasmic reticulum (ER) stress is the one receiving much interest in recent years [9, 27].

Disturbed homeostasis in the ER lumen will result in ER stress and initiate the unfolded protein response (UPR). The latter process is a mechanism promoting survival of cells impaired by ER stress. However, when the UPR adaption to ER stress fails, the prolonged UPR can cause tissue injuries and organ dysfunction [26]. In kidney disorders, accumulating evidence suggests a pathophysiological role of ER stress [9]: inflammation and oxidative stress compounded by ER stress contribute to glomerular and tubular damages in patients with acute kidney disease [9]. Based on these studies, the artificial modulation of ER stress has become a novel therapeutic strategy for protection of renal cells. For example, cells with GRP78 overexpression were resistant to symptoms associated with ER stress [16]. Induced production of ORP150 also attenuated impairments associated with kidney injuries [2]. Moreover, chemical compounds modulating ER stress have also shown promising treatment efficiency for diseases due to ER stress augmentation. In the study of Asmellash *et al*., the authors employed trans-4,5-dihydroxy-1,2-dithiane (DTTox) to protect the proximal tubular epithelium against a nephrotoxic chemical by stimulating the expression of GRP78 [1]. Except for GRP78, the N-termini of transmembrane ER proteins such as inositol-requiring enzyme-1 (IRE1), double-stranded RNA-activated protein kinase-like ER kinase (PERK), and activating transcription factor-6 (ATF6) are all crucial members involved in the transition of the UPR from pro-survival to pro-apoptosis. In the current study, we selected STF-083010, an inhibitor of XBP1 splicing caused by IRE1, as the treatment modality for ER stress-induced impairments in ARF rats. The compound was first identified by Papandreou *et al*. in 2016 [17] and it was shown that the agent specifically inhibited the endonuclease activity of IRE1 without affecting its kinase function [13]. The endonuclease activity of IRE1 promotes the removal of a 26-nucleotide intron from the *XBP1* mRNA and generates *XBP1*s, the activated form of *XBP1*. Moreover, STF-083010 has shown its potential to effectively control ER stress-induced disorders [17, 28]. The compound was intraperitoneally injected into kidneys of IR-injured rats and the effect of the administration was assessed by determining the changes in renal function and structure as well as the production of indicators of inflammation and oxidative stress. Moreover, the activities of UPR members and caspase 3 were also detected in the current study. The findings outlined indicated that the administration of STF-083010 was capable of attenuating ARF by suppressing ER stress-induced apoptosis and inflammation.

Materials and Methods

Antibodies and reagents

An antibody against GRP78 (cat. no. D151791) was purchased from Sangon Biotech (Shanghai, China). Antibodies against phosphorylated IRE1 (p-IRE1) (cat. no. ab48187) and the spliced form of XBP1 (XBP1s) (cat. no. ab37152) were purchased from Abcam (Cambridge, MA, USA). Antibodies against total IRE1 (t-IRE1) (cat. no. bs-8680R) and β-actin (bsm-33139M) were purchased from Bioss (Beijing, China). An antibody against CHOP (cat. no. 15204–1-AP) was purchased from Proteintech Group, Inc. (Wuhan, China). Antibody against cleaved caspase 3 was purchased from Cell Signaling Technology (Danvers, MA, USA ; cat. no. #9661) (US). Secondary goat anti-rabbit (cat. no. A0208) and goat anti-mouse (cat. no. A0216) IgG-HRP antibodies were purchased from Beyotime Biotechnology (Shanghai,

China). RIPA lysis buffer (cat. no. P0013B) and a protein concentration detection kit using the BCA method (cat. no. P0009) were obtained from Beyotime Biotechnology (Shanghai, China). An RNApure High-purity Total RNA Rapid Extraction Kit (cat. no. RP1201) and Super M-MLV Reverse Transcriptase (cat. no. PR6502) were purchased from BioTeke (Beijing, China). An In Situ Cell Death Detection Kit (cat. no. 11684817910) was purchased from Roche Group (Switzerland). Detection kits for creatinine (Cr) (cat. no. C011-2), blood urea nitrogen (BUN) (cat. no. C013-1), malondialdehyde (MDA) (cat. no. A003-1), glutathione (GSH) (cat. no. A006-2), glutathione peroxidase (GSH-x) (cat. no. A005), superoxide dismutase (SOD) (cat. no. A001-1), and myeloperoxidase (MPO) (cat. no. A044) were purchased from Nanjing Jiancheng Bioengineering Institute (Nanjing, China). A Bradford Protein Assay Kit (cat. no. P0006) was purchased from Beyotime Biotechnology (Shanghai, China). An ELISA kit for detection of tumor necrosis factor α (TNF-α) (cat. no. EK0526) was purchased from Boster Biological Technology Co., Ltd. (Wuhan, China). An ELISA kit for detection of interleukin 1β (IL-1β) (cat. no. EK301B1/2) was purchased from Hangzhou Multi Sciences (Hangzhou, China). STF-083010 (cat. no. HY-15845) (purity>98.0%) was purchased from MedChemExpress (Monmouth Junction, NJ, USA). DMSO (cat. no. D103272-500ml) (purity>99%) was purchased from Aladdin (Shanghai, China).

Animals

Adult male Sprague Dawley (SD) rats (eight week old, weighing 200–300 g) were obtained from Changsheng Biotechnology Inc. (Benxi, China). The rats were housed in cages at room temperature (22 ± 1°C) and a constant humidity (65–75%) with food and water available and a 12:12-h light-dark cycle. All the procedures with animals were conducted in accordance with the Animal Care Guidelines of the Institutional Animal Ethics Committee of Shandong University.

IR-induced ARF model and administration of STF-083010

Twenty-four SD rats were randomly divided into four groups (six for each group). For rats in the Mock (rats received injection of DMSO, the vehicle for STF-083010) and STF-083010 (rats receiving treatment with STF-083010) groups, 10% DMSO (0.5 ml) or 15 mg/kg STF-083010 were intraperitoneally injected 1 h before model induction based on the study of Zhao *et al*. [28]. Then rats were then anesthetized with an intraperitoneal injection of 50 mg/kg pentobarbital sodium and placed on an operating bench in the prone position. After a midabdominal laparotomy, the kidneys were exposed, and the renal pedicles were clamped with atraumatic vascular clamps for 40 min. Then the clamps were removed and the injury was sutured for reperfusion for 24 h. Upon completion of reperfusion, the rats were anesthetized with 50 mg/kg pentobarbital sodium and blood was collected from eye balls. Then the rats were sacrificed, and renal tissues were collected and preserved at −80°C for subsequent assays (one kidney of a rat was used for histopathology and immunostaining, and the other one was used for biochemical, RT-PCR, and western blotting detections). For rats in the sham group, the operation was performed only without clamping of the renal pedicles. Moreover, the effect of another IRE1 inhibitor, 4μ8C, on attenuation of IR injury-induced renal injuries was also detected, and it is shown in the supplementary data.

Detection of renal function and structure

Renal tissues were collected from rats in different groups and subjected to hematoxylin and eosin (H&E) and TUNEL staining. For H&E staining, tissues were placed into Bouin solution (4% formaldehyde) for perfusion fixation, dehydrated using different concentrations of alcohol, and vitrified in dimethylbenzene. Then samples were embedded in paraffin, sectioned, and stained with H&E. The results were detected under a microscope (BX53, Olympus, Tokyo, Japan), and the images were captured by a digital microscope camera (DP73, Olympus, Tokyo, Japan) at 400× magnification. TUNEL staining was performed using an In Situ Cell Death Detection Kit according to manufacturer's instructions, and the results were detected under 400× magnification. The apoptotic rate was equal to the averaged ratio of the TUNEL-positive cell number to the total cell number in five randomly selected fields. The function of the kidney was detected by measuring the levels of Cr and BUN in plasma using detecting kits following the procedures in the manufacturer's instructions.

Detection of oxidative stress

The levels of MDA, GSH, GSH-x, and SOD were determined using detecting kits according to the manufacturers' instructions.

Detection of inflammatory response

The levels of TNF-α and IL-1β were measured using ELISA kits according to the manufacturers' instructions. The production of MPO was measured using an MPO detection kit (Nanjing Jiancheng Bioengineering Institute) according to the manufacturer's instructions.

Reverse transcription PCR (RT-PCR)

Total RNA was extracted with an RNApure High-purity Total RNA Rapid Extraction Kit according to the manufacturer's instructions and was subjected to reverse transcription using Super M-MLV Reverse Transcriptase to achieve cDNA templates for PCR. The reaction mixture for PCR contained 10 μl Taq PCR Master Mix, 1 μl of each primer (for *XBP1*s, 5′-TGGGCATCTCAAACCTGCTT-3′, forward, and 5′-GGAGTGGTCTGTACCAAGTGGA-3′, backward; for unspliced *XBP1* (*XBP1*u), 5′-CATGGGCTTGTGATTGAGAA-3′, forward, 5′-TGCAGAGGCGCACGTAGT-3′, backward; for *β-actin*, 5′-GGAGATTACTGCCCTGGCTCCTAGC-3′, forward, 5′-GGCCGGACTCATCGTACTCCTGCTT-3′, backward), 1 μl cDNA template, and 7 μl ddH_2O. The amplification was performed with the following thermal cycling parameters: a denaturation was performed at 95°C for 5 min followed by 36 cycles of amplification at 95°C for 20 s, 52°C for 20 s, and 72°C for 30 s; the reaction was then stopped at 25°C for 5 min. The PCR products were subjected to agarose gel electrophoresis (WD-9413B, Liuyi Factory, Beijing, China), and the ratio of XBP1s to XBP1u was calculated based on the results of grey values of bands.

Immunochemical detection

The renal tissues were hydrated with different concentrations of alcohol (70% for 2 h, 80% overnight, 90% for 2 h, 100% for 2 h, and 100% for 2h) and fixed with dimethylbenzene for 30 min. After incubation in antigen retrieval buffers for 30 min, the sections were placed in 3% H_2O_2 for 15 min and washed with PBS for three times. Then the sections were incubated with primary antibodies against CHOP (1:200) and XBP1s (1:200) at 4°C overnight. After three washes with PBS, secondary antibodies (1:200) were added and incubated with sections for 30 min at 37°C. Thereafter, the sections were incubated with HRP-labeled avidin for 30 min at 37°C and reacted with DAB. The sections were restained with hematoxylin and dehydrated. The results were detected by scanning the sections using a microscope (BX53, Olympus, Tokyo, Japan) at 400× magnification.

Western blotting

Tissues were lysed using 1% PMSF, and total cellular protein was collected by centrifugation at 10,000 × g for 10 min. Thirty micrograms of protein from different samples were subjected to 10% sodium dodecyl sulfate polyacrylamide gel electrophoresis (SDS-PAGE) at 80 V for 2.5 h. The proteins were transferred onto polyvinylidene difluoride (PVDF) membranes and rinsed with TTBS. Then the membranes were blocked with skimmed milk solution for 1 h and incubated with the primary antibodies against GRP78 (1:500), p-IRE1 (1:1,000), t-IRE1 (1:500), XBP1s (1:1,000), CHOP (1:500), cleaved caspase 3 (1:500), and β-actin (1:5,000) at 4°C overnight. Secondary HRP-conjugated IgG antibodies (1:500) were added onto the membranes and incubated for 45 min at 37°C. After a final six washes with TTBS, the blots were developed using the Beyo ECL Plus reagent, and the images were recorded with a Gel Imaging System. The relative expression levels of proteins were calculated with Gel-Pro Analyzer (Media Cybernetics, Rockville, MD, USA).

Statistical analysis

The data were expressed as the mean ± standard deviation (n=6). One-way ANOVA and post hoc multiple comparisons using Fisher's Least Significant Difference (LSD) test were performed with a significance level of 0.05 (two-tailed *P* value). All the statistical analyses and graph manipulations were conducted using GraphPad Prism version 6.0 (GraphPad Software, Inc., San Diego, CA, USA).

Results

Administration of STF-083010 ameliorated kidney structure and function in ARF rats

Renal morphology was evaluated with H&E staining, and the results are shown in Fig. 1A. Twenty-four hours after the surgery, severe interstitial edema, cellular infiltration, and tubular cell structure deterioration could be clearly observed in the Model and Mock groups, which represented progressive damages in the kidneys. However, in the STF-083010 group, only mild tubular damage with no tubular necrosis and inflammatory cell infiltration could be observed. The pattern of changes was similar for apoptosis detection with TUNEL stain-

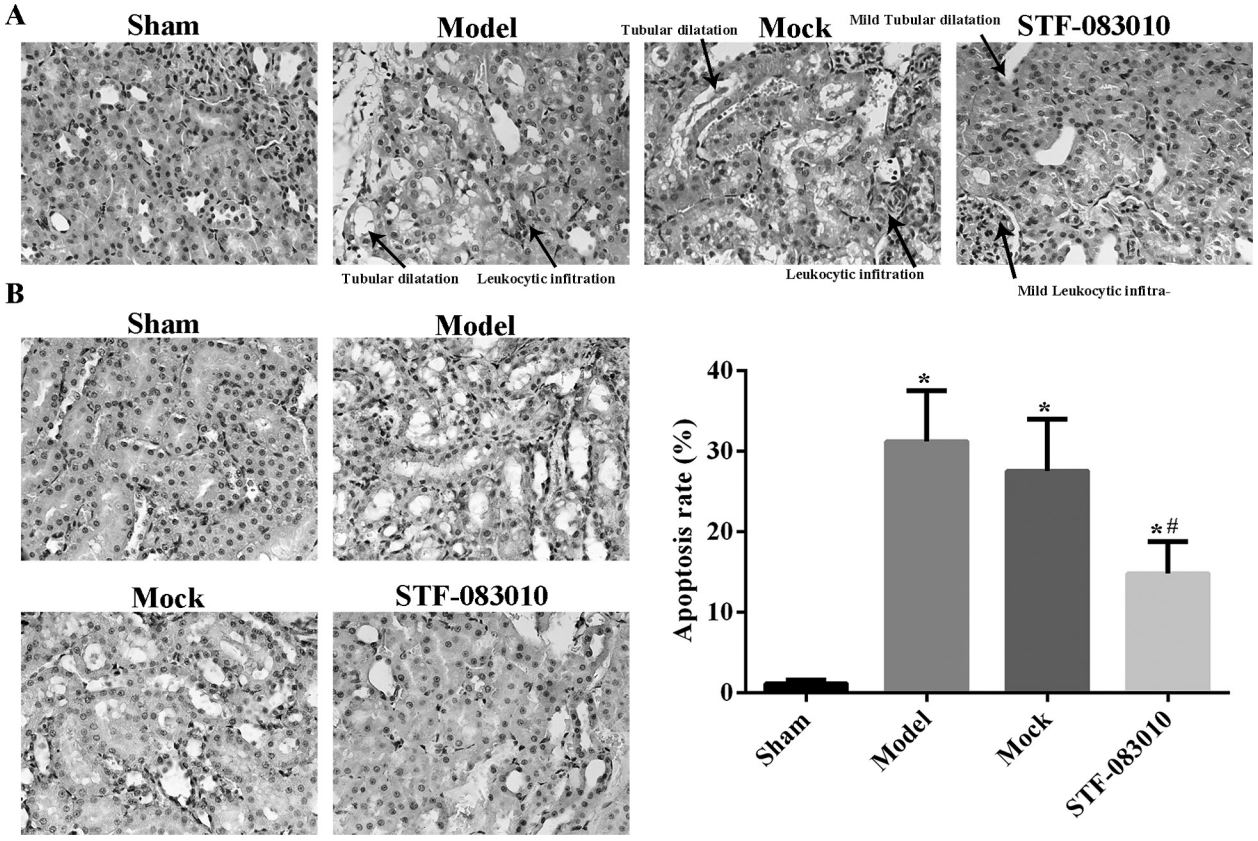

Fig. 1. Effect of STF-083010 administration on the histological structure of ARF kidneys (n=6). In the photomicrograph of rat kidney tissues with H&E staining (A) (400×), it can be seen that establishment of the ARF model induced tubular dilation and leukocytic infiltration in kidney tissues but that administration of STF-083010 was able to alleviate the impairments induced by IR injury. The results of TUNEL staining (B) (400×) showed that establishment of the ARF model increased the apoptotic cell (stained brown) number and that administration of STF-083010 was able to inhibit apoptosis in kidney tissues. **P*<0.001 vs. Sham. #*P*<0.001 vs. Model. Sham group, rats underwent exposure of kidneys without clamping. Model group, rats underwent induction of ARF by clamping. Mock group, ARF rats receiving injection of DMSO. STF-083010 group, ARF rats receiving treatment with STF-0830101.

ing: fewer apoptotic cells (stained brown) were recorded in the STF-083010 group when compared with the Model and Mock groups, and the differences were statistically significant (Fig. 1B) (P<0.001). A similar renal protecting effect was also observed when the rats were treated with another IRE1 inhibitor, 4μ8C (Supplementary Fig. S1), indicating that the effect of STF-083010 was exerted specifically by inhibiting IRE1. The levels of plasma Cr and BUN were elevated in rats subjected to the ligation operation (Fig. 2 and Supplementary Table S1) compared with the levels of those in the Sham group: the levels of the two indicators were reversed by the pretreatment with STF-083010 (Fig. 2 and Supplementary Table S1). Taken together, it was concluded that the administration of STF-083010 evidently attenuated impairments due to IR injury both in renal structure and function.

Administration of STF-083010 attenuated oxidative stress induced by ARF in kidney tissues

To characterized the effect of STF-083010 on the level of oxidative stress induced by IR injury, the tissue levels of MDA, GSH, GSH-x, and SOD were quantified with specific kits. As shown in Fig. 3 and Supplementary Table S1, the establishment of the ARF model increased the MDA production in the kidneys, whereas it suppressed the production of antioxidative factors, including GSH, GSH-x, and SOD, which promoted oxidative stress. Once the ARF rats were pretreated with STF-083010, the triggered oxidative stress in IR-injured kidneys was dramatically suppressed, represented by the decreased level of MDA and increased levels of GSH,

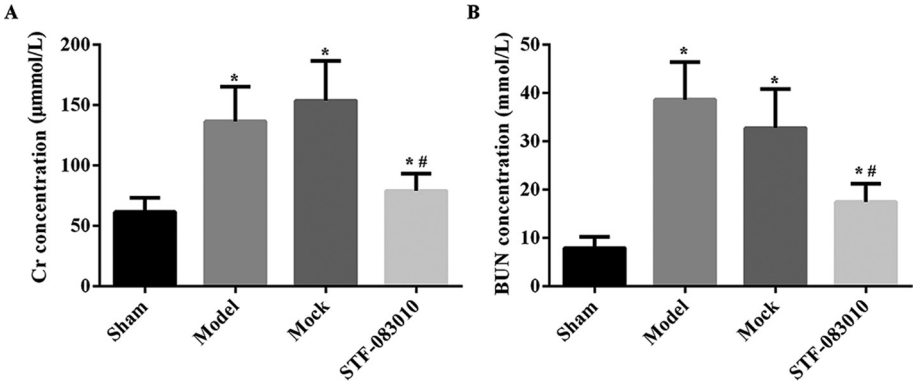

Fig. 2. Effect of STF-083010 administration on the function of ARF kidneys (n=6). Based on the statistical analyses, induction of the ARF model increased the levels of Cr (A) and BUN (B). Administration of STF-083010 was able to restore the levels of Cr (A) and BUN (B) to a relatively normal level. **P*<0.001 vs. Sham. #*P*<0.001 vs. Model. Sham group, rats underwent exposure of kidneys without clamping. Model group, rats underwent induction of ARF by clamping. Mock group, ARF rats receiving injection of DMSO. STF-083010 group, ARF rats receiving treatment with STF-0830101.

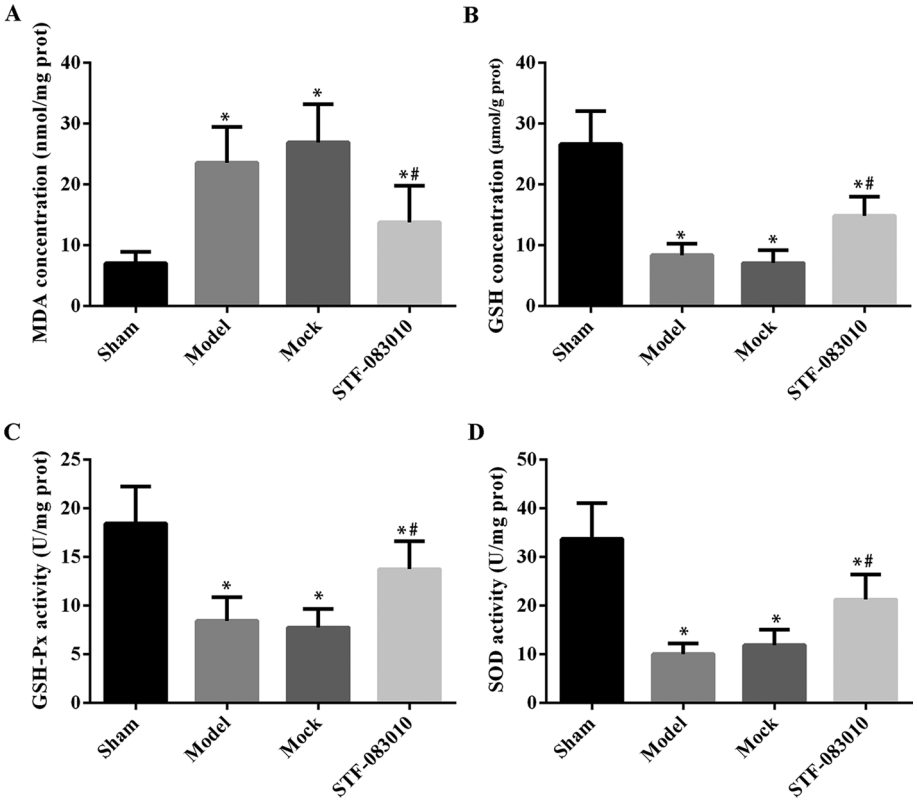

Fig. 3. Effect of STF-083010 administration on oxidative stress of ARF kidneys (n=6). Based on the statistical analyses, the induction of ARF model increased the level of MDA (A), whereas it suppressed the levels of GSH (B), GSH-Px (C), and SOD (D). Administration of STF-083010 was able to decrease the level of MAD (A) and increase the levels of GSH (B), GSH-Px (C), and SOD (D). **P*<0.001 vs. Sham. #*P*<0.001 vs. Model. Sham group, rats underwent exposure of kidneys without clamping. Model group, rats underwent induction of ARF by clamping. Mock group, ARF rats receiving injection of DMSO. STF-083010 group, ARF rats receiving treatment with STF-0830101.

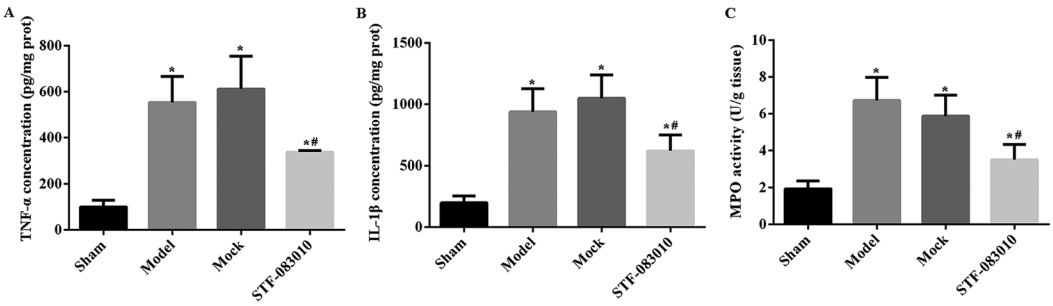

Fig. 4. Effect of STF-083010 administration on the inflammatory response of ARF kidneys (n=6). Based on the statistical analyses, induction of the ARF model increased the levels of TNF-α (A), IL-1β (B), and MPO (C), while the administration of STF-083010 suppressed the levels of the three indicators. **P*<0.001 vs. Sham. $^{\#}P$<0.001 vs. Model. Sham group, rats underwent exposure of kidneys without clamping. Model group, rats underwent induction of ARF by clamping. Mock group, ARF rats receiving injection of DMSO. STF-083010 group, ARF rats receiving treatment with STF-0830101.

GSH-x, and SOD (Fig. 3 and Supplementary Table S1) (*P*<0.001).

Administration of STF-083010 attenuated inflammation induced by ARF in kidney tissues

The levels of pro-inflammatory cytokines, TNF-α and IL-1β, were increased in the Model and Mock groups compared with the Sham group (Figs. 4A, B and Supplementary Table S1) (*P*<0.001). Administration of STF-083010 attenuated the increase in TNF-α and IL-1β in ARF rats, indicating an anti-inflammatory effect. Similarly, the renal MPO level was higher in the Model and Mock groups when compare with the Sham group, which indicated the infiltration of neutrophils in IR-injured renal tissues (Fig. 4C and Supplementary Table S1) (*P*<0.001). The administration of STF-083010 abolished the MPO activity induced by IR injury (Fig. 4C and Supplementary Table S1).

Administration of STF-083010 suppressed the prolonged UPR induced by ARF in kidney tissues

To validate our hypothesis that STF-083010 exerted its anti-ARF function by suppressing ER stress, the expressions of members involved in UPR initiation were detected. The upregulated expressions of GRP78, p-IRE1, XBP1s, and CHOP due to induction of ARF were suppressed by the pretreatment with STF-083010 (Fig. 5A). The ratio of the *XBP1*s mRNA level to the *XBP1*u mRNA level was first increased by IR injury and then decreased by the administration of STF-083010, which indicated that the endonuclease activity of IRE1 was inhibited by STF-083010 (Fig. 5B). Moreover, the downstream signaling of the IRE1/XBP1 pathway was proved to be blocked by STF-083010: the expression of cleaved caspase 3 was inhibited in the STF-083010 group when compared with the Model and Mock groups (Fig. 5A). The suppressing effect of STF-083010 on XBP1 splicing and CHOP expression was further validated by immunochemical staining (Figs. 5C and D). Taken together, STF-083010 was capable of inhibiting IR injury-induced apoptosis and inflammation in renal tissues by blocking IRE1/XBP1 signaling.

Discussion

STF-083010 was identified to be an effective inhibitor for the endonuclease activity of IRE1 [13], and its potential to treat disorders related to a prolonged UPR has been validated [13, 14, 17]. In the current study, we employed STF-083010 as an alternative treatment modality against IR injury-induced ARF and found that the agent exhibited a considerably protective effect on renal tissues. Pretreatment with STF-083010 was able to alleviate impairments in renal structure and function, and this was accompanied by the decreased cell apoptosis and production of pro-inflammatory cytokines in ARF rats. As expected, the effect of STF-083010 on the kidneys was associated with the suppressed pro-apoptotic and pro-inflammatory effect of the UPR, represented by downregulated expressions of GRP78, p-IRE1, XBP1s, CHOP, and cleaved caspase 3.

The ER is an important organelle for the synthesis and folding of secreted, membrane-bound, and some organelle-targeted proteins [21]. In some extreme environ-

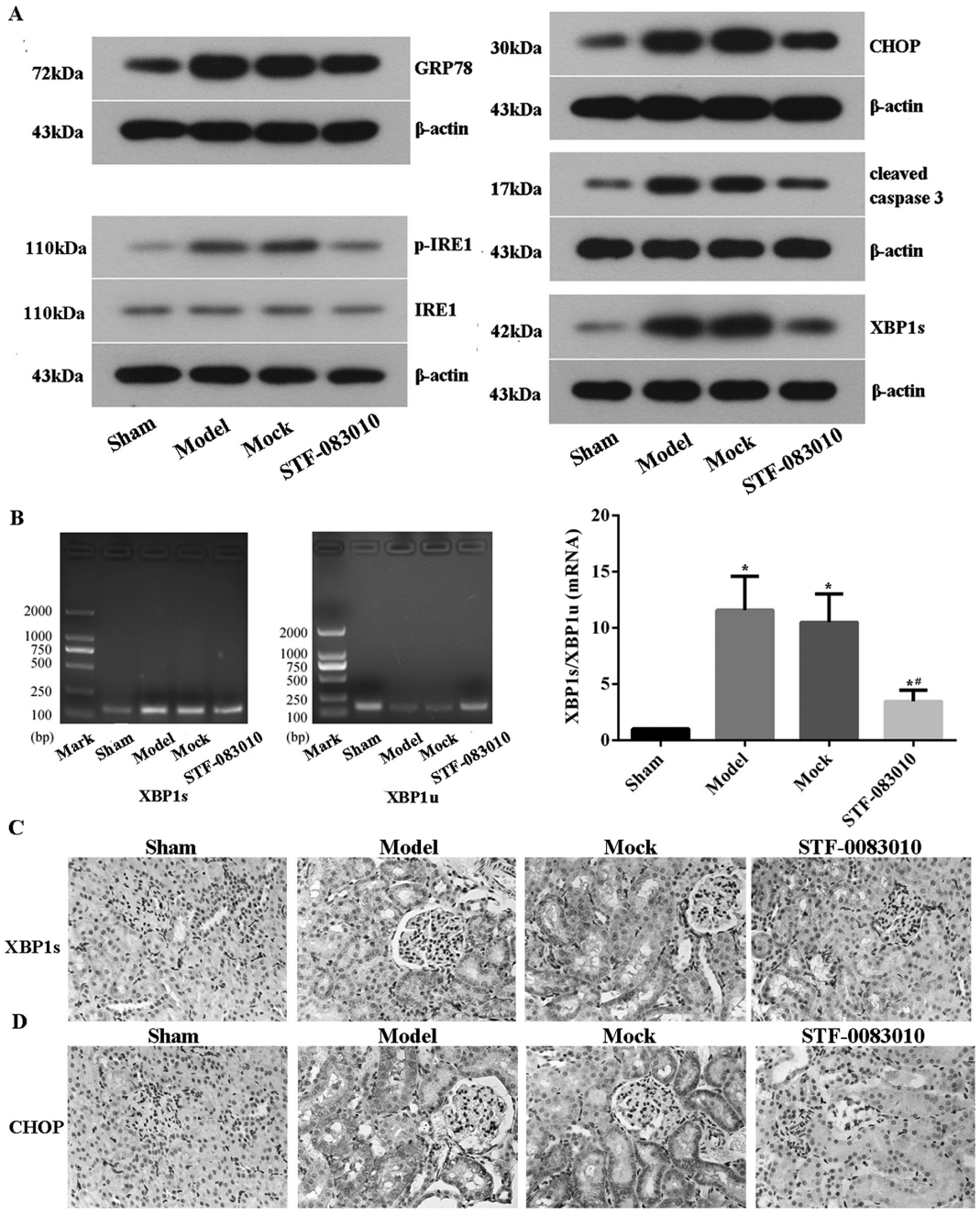

Fig. 5. Effect of STF-083010 administration on ER stress of ARF kidneys (n=6). As illustrated by western blotting, establishment of the ARF model increased the expressions of GRP78, p-IRE, XBP1s, CHOP (A–C) and the activity of caspase 3 (A). The expression patterns of the above indicators were reversed by the administration of STF-083010. **P*<0.001 vs. Sham. #*P*<0.001 vs. Model. Sham group, rats underwent exposure of kidneys without clamping. Model group, rats underwent induction of ARF by clamping. Mock group, ARF rats receiving injection of DMSO. STF-083010 group, ARF rats receiving treatment with STF-0830101.

ments, the protein folding capability of the ER will be disturbed, which results in the accumulation of unfolded proteins–a condition termed ER stress. Aggregation of unfolded proteins is toxic to cells, and numerous pathophysiological conditions are attributed to ER stress, including ischemia, neurodegenerative diseases, and diabetes [11]. Regarding kidney diseases, ER stress plays multiple pathogenic roles. For example, previous studies

have identified an increased ER stress level in podocytes in Heymann nephritis [6, 7]: it was found that the complement-mediated podocyte injuries induced the expression of ER chaperones such as GRP78 and GRP94, which represented an adaptive UPR pathway [6, 7]. In the study of Inagi *et al*., mesangial injuries in rats induced the UPR pathway in glomeruli and attenuated protein translation via the PERK/eIF2α pathway [10]. In the current study, the ARF model initiated the UPR by increasing the expressions of GRP78, p-IRE1, and XBP1s and promoted a prolonged UPR transformed from pro-survival to pro-apoptosis and pro-inflammation, which was represented by the upregulated levels of inflammatory cytokines, CHOP, and cleaved caspase 3.

The IRE1/XBP1 pathway is a complex cellular response mediating the progression of the UPR. IRE1 is a dual-activity enzyme with a serine–threonine kinase domain and an endoribonuclease domain [4]. Once activated during the UPR, the endonuclease activity of IRE1 will promote the removal of a 26-nucleotide intron from the *XBP1* mRNA and generate *XBP1*s [25]. During a prolonged UPR, IRE1 can trigger pro-apoptotic pathways by activating downstream molecules such as CHOP [21]. XBP1s is a molecule with multiple targets, and it will not only induce pro-apoptotic signaling sequence by activating $P58^{IPK}$ that promotes the expression of CHOP [12, 24] but will also promote inflammation by mediating NF-κB activation [22]. Moreover, ER chaperones have also been found to be regulated by XBP1s in a positive feedback loop [21]. CHOP is also defined as growth arrest- and DNA-damage inducible gene 153 (GADD153) and induces apoptosis under ER stress by regulating BCL2, GADD34, endoplasmic reticulum oxidoreductin 1 (ERO1α), and Tribbles-related protein 3 (TRB3) [21]. CHOP deficiency will result in reduced cleavage of caspase 3 as well [23]. In the present study, the increased expressions of GRP78, p-IRE1, XBP1s, and CHOP were inhibited by the administration of STF-083010, further inhibiting the apoptosis and inflammation associated with the prolonged UPR. It was inferred that the administration of STF-083010 blocked the splicing of *XBP1* by IRE1 and resulted in the suppression of CHOP-related apoptosis and NF-κB-related inflammation, which eventually converged as a ARF attenuating effect.

In conclusion, the current study evaluated the renal protective effect of STF-083010 for the first time. Pretreatment with the agent improved the renal structure and function in AFR rats by blocking ER stress-induced apoptosis and inflammation. Although the study only performed a few assays to reveal the mechanism associated with the treatment effect of STF-083010, it clearly showed that the inhibition of splicing of *XBP1* by STF-083010 could serve as a promising therapeutic strategy in ARF treatment. More comprehensive work regarding the mechanism and possible side effects associated with STF-083010 treatment will be performed to facilitate the practical application of the agent in the clinic.

Acknowledgments

This study was supported by grants from the Jining Science and Technology Development Project (No. 2014jnnk04) and the Science and Technology Development Project for Medicine and Health of Shandong Province (No. 2017WS512).

References

1. Asmellash, S., Stevens, J.L., and Ichimura, T. 2005. Modulating the endoplasmic reticulum stress response with trans-4,5-dihydroxy-1,2-dithiane prevents chemically induced renal injury in vivo. *Toxicol. Sci.* 88: 576–584. [Medline] [CrossRef]
2. Bando, Y., Tsukamoto, Y., Katayama, T., Ozawa, K., Kitao, Y., Hori, O., Stern, D.M., Yamauchi, A., and Ogawa, S. 2004. ORP150/HSP12A protects renal tubular epithelium from ischemia-induced cell death. *FASEB J.* 18: 1401–1403. [Medline] [CrossRef]
3. Boros, P. and Bromberg, J.S. 2006. New cellular and molecular immune pathways in ischemia/reperfusion injury. *Am. J. Transplant.* 6: 652–658. [Medline] [CrossRef]
4. Chen, Y. and Brandizzi, F. 2013. IRE1: ER stress sensor and cell fate executor. *Trends Cell Biol.* 23: 547–555. [Medline] [CrossRef]
5. Chertow, G.M., Levy, E.M., Hammermeister, K.E., Grover, F., and Daley, J. 1998. Independent association between acute renal failure and mortality following cardiac surgery. *Am. J. Med.* 104: 343–348. [Medline] [CrossRef]
6. Cybulsky, A.V., Takano, T., Papillon, J., and Bijian, K. 2005. Role of the endoplasmic reticulum unfolded protein response in glomerular epithelial cell injury. *J. Biol. Chem.* 280: 24396–24403. [Medline] [CrossRef]
7. Cybulsky, A.V., Takano, T., Papillon, J., Khadir, A., Liu, J., and Peng, H. 2002. Complement C5b-9 membrane attack complex increases expression of endoplasmic reticulum stress proteins in glomerular epithelial cells. *J. Biol. Chem.* 277: 41342–41351. [Medline] [CrossRef]
8. He, L., Peng, X., Zhu, J., Chen, X., Liu, H., Tang, C., Dong, Z., Liu, F., and Peng, Y. 2014. Mangiferin attenuate sepsis-induced acute kidney injury via antioxidant and anti-inflammatory effects. *Am. J. Nephrol.* 40: 441–450. [Medline]

[CrossRef]
9. Inagi, R. 2009. Endoplasmic reticulum stress in the kidney as a novel mediator of kidney injury. *Nephron, Exp. Nephrol.* 112: e1–e9. [Medline] [CrossRef]
10. Inagi, R., Kumagai, T., Nishi, H., Kawakami, T., Miyata, T., Fujita, T., and Nangaku, M. 2008. Preconditioning with endoplasmic reticulum stress ameliorates mesangioproliferative glomerulonephritis. *J. Am. Soc. Nephrol.* 19: 915–922. [Medline] [CrossRef]
11. Kaufman, R.J. 2002. Orchestrating the unfolded protein response in health and disease. *J. Clin. Invest.* 110: 1389–1398. [Medline] [CrossRef]
12. Lee, A.H., Iwakoshi, N.N., and Glimcher, L.H. 2003. XBP-1 regulates a subset of endoplasmic reticulum resident chaperone genes in the unfolded protein response. *Mol. Cell. Biol.* 23: 7448–7459. [Medline] [CrossRef]
13. Ming, J., Ruan, S., Wang, M., Ye, D., Fan, N., Meng, Q., Tian, B., and Huang, T. 2015. A novel chemical, STF-083010, reverses tamoxifen-related drug resistance in breast cancer by inhibiting IRE1/XBP1. *Oncotarget* 6: 40692–40703. [Medline] [CrossRef]
14. Mohammed-Ali, Z., Cruz, G.L., and Dickhout, J.G. 2015. Crosstalk between the unfolded protein response and NF-κB-mediated inflammation in the progression of chronic kidney disease. *J. Immunol. Res.* 2015: 428508. [Medline] [CrossRef]
15. Molitoris, B.A., and Marrs, J. 1999. The role of cell adhesion molecules in ischemic acute renal failure. *Am. J. Med.* 106: 583–592. [Medline] [CrossRef]
16. Morris, J.A., Dorner, A.J., Edwards, C.A., Hendershot, L.M., and Kaufman, R.J. 1997. Immunoglobulin binding protein (BiP) function is required to protect cells from endoplasmic reticulum stress but is not required for the secretion of selective proteins. *J. Biol. Chem.* 272: 4327–4334. [Medline] [CrossRef]
17. Papandreou, I., Denko, N.C., Olson, M., Van Melckebeke, H., Lust, S., Tam, A., Solow-Cordero, D.E., Bouley, D.M., Offner, F., Niwa, M., and Koong, A.C. 2011. Identification of an Ire1alpha endonuclease specific inhibitor with cytotoxic activity against human multiple myeloma. *Blood* 117: 1311–1314. [Medline] [CrossRef]
18. Sáenz-Morales, D., Escribese, M.M., Stamatakis, K., García-Martos, M., Alegre, L., Conde, E., Pérez-Sala, D., Mampaso, F., and García-Bermejo, M.L. 2006. Requirements for proximal tubule epithelial cell detachment in response to ischemia: role of oxidative stress. *Exp. Cell Res.* 312: 3711–3727. [Medline] [CrossRef]
19. Sahu, B.D., Kuncha, M., Sindhura, G.J., and Sistla, R. 2013. Hesperidin attenuates cisplatin-induced acute renal injury by decreasing oxidative stress, inflammation and DNA damage. *Phytomedicine* 20: 453–460. [Medline] [CrossRef]
20. Semedo, P., Palasio, C.G., Oliveira, C.D., Feitoza, C.Q., Gonçalves, G.M., Cenedeze, M.A., Wang, P.M.H., Teixeira, V.P.A., Reis, M.A., Pacheco-Silva, A., and Câmara, N.O. 2009. Early modulation of inflammation by mesenchymal stem cell after acute kidney injury. *Int. Immunopharmacol.* 9: 677–682. [Medline] [CrossRef]
21. Szegezdi, E., Logue, S.E., Gorman, A.M., and Samali, A. 2006. Mediators of endoplasmic reticulum stress-induced apoptosis. *EMBO Rep.* 7: 880–885. [Medline] [CrossRef]
22. Tam, A.B., Mercado, E.L., Hoffmann, A., and Niwa, M. 2012. ER stress activates NF-κB by integrating functions of basal IKK activity, IRE1 and PERK. *PLoS One* 7: e45078. [Medline] [CrossRef]
23. Tamaki, N., Hatano, E., Taura, K., Tada, M., Kodama, Y., Nitta, T., Iwaisako, K., Seo, S., Nakajima, A., Ikai, I., and Uemoto, S. 2008. CHOP deficiency attenuates cholestasis-induced liver fibrosis by reduction of hepatocyte injury. *Am. J. Physiol. Gastrointest. Liver Physiol.* 294: G498–G505. [Medline] [CrossRef]
24. Yan, W., Frank, C.L., Korth, M.J., Sopher, B.L., Novoa, I., Ron, D., and Katze, M.G. 2002. Control of PERK eIF2α kinase activity by the endoplasmic reticulum stress-induced molecular chaperone P58IPK. *Proc. Natl. Acad. Sci. USA* 99: 15920–15925. [Medline] [CrossRef]
25. Yoshida, H., Matsui, T., Yamamoto, A., Okada, T., and Mori, K. 2001. XBP1 mRNA is induced by ATF6 and spliced by IRE1 in response to ER stress to produce a highly active transcription factor. *Cell* 107: 881–891. [Medline] [CrossRef]
26. Zha, X., Yue, Y., Dong, N., and Xiong, S. 2015. Endoplasmic reticulum stress aggravates viral myocarditis by raising inflammation through the IRE1-associated NF-κB pathway. *Can. J. Cardiol.* 31: 1032–1040. [Medline] [CrossRef]
27. Zhang, K. and Kaufman, R.J. 2008. From endoplasmic-reticulum stress to the inflammatory response. *Nature* 454: 455–462. [Medline] [CrossRef]
28. Zhao, W., Han, F., and Shi, Y. 2016. IRE1α pathway of endoplasmic reticulum stress induces neuronal apoptosis in the locus coeruleus of rats under single prolonged stress. *Prog. Neuropsychopharmacol. Biol. Psychiatry* 69: 11–18. [Medline] [CrossRef]
29. Zuk, A. and Bonventre, J.V. 2016. Acute kidney injury. *Annu. Rev. Med.* 67: 293–307. [Medline] [CrossRef]